

Raitzer, David A.; Drouard, Joeffrey

Working Paper

Empirically estimated impacts of climate change on global crop production via increasing precipitation-evapotranspiration extremes

ADB Economics Working Paper Series, No. 759

Provided in Cooperation with:

Asian Development Bank (ADB), Manila

Suggested Citation: Raitzer, David A.; Drouard, Joeffrey (2024) : Empirically estimated impacts of climate change on global crop production via increasing precipitation-evapotranspiration extremes, ADB Economics Working Paper Series, No. 759, Asian Development Bank (ADB), Manila, <https://doi.org/10.22617/WPS240589-2>

This Version is available at:

<https://hdl.handle.net/10419/310398>

Standard-Nutzungsbedingungen:

Die Dokumente auf EconStor dürfen zu eigenen wissenschaftlichen Zwecken und zum Privatgebrauch gespeichert und kopiert werden.

Sie dürfen die Dokumente nicht für öffentliche oder kommerzielle Zwecke vervielfältigen, öffentlich ausstellen, öffentlich zugänglich machen, vertreiben oder anderweitig nutzen.

Sofern die Verfasser die Dokumente unter Open-Content-Lizenzen (insbesondere CC-Lizenzen) zur Verfügung gestellt haben sollten, gelten abweichend von diesen Nutzungsbedingungen die in der dort genannten Lizenz gewährten Nutzungsrechte.

Terms of use:

Documents in EconStor may be saved and copied for your personal and scholarly purposes.

You are not to copy documents for public or commercial purposes, to exhibit the documents publicly, to make them publicly available on the internet, or to distribute or otherwise use the documents in public.

If the documents have been made available under an Open Content Licence (especially Creative Commons Licences), you may exercise further usage rights as specified in the indicated licence.



<https://creativecommons.org/licenses/by/3.0/igo/>

EMPIRICALLY ESTIMATED IMPACTS OF CLIMATE CHANGE ON GLOBAL CROP PRODUCTION VIA INCREASING PRECIPITATION- EVAPOTRANSPIRATION EXTREMES

David A. Raitzer and Joeffrey Drouard

NO. 759

December 2024

**ADB ECONOMICS
WORKING PAPER SERIES**

ADB Economics Working Paper Series

Empirically Estimated Impacts of Climate Change on Global Crop Production via Increasing Precipitation–Evapotranspiration Extremes

David A. Raitzer and Joeffrey Drouard

No. 759 | December 2024

David A. Raitzer (draitzer@adb.org) is a senior economist at the Economic Research and Development Impact Department, Asian Development Bank. Joeffrey Drouard (joeffrey.drouard@univ-cotedazur.fr) is an associate professor at the Université Côte d'Azur.

The *ADB Economics Working Paper Series* presents research in progress to elicit comments and encourage debate on development issues in Asia and the Pacific. The views expressed are those of the authors and do not necessarily reflect the views and policies of ADB or its Board of Governors or the governments they represent.



Creative Commons Attribution 3.0 IGO license (CC BY 3.0 IGO)

© 2024 Asian Development Bank
6 ADB Avenue, Mandaluyong City, 1550 Metro Manila, Philippines
Tel +63 2 8632 4444; Fax +63 2 8636 2444
www.adb.org

Some rights reserved. Published in 2024.

ISSN 2313-6537 (print), 2313-6545 (PDF)
Publication Stock No. WPS240589-2
DOI: <http://dx.doi.org/10.22617/WPS240589-2>

The views expressed in this publication are those of the authors and do not necessarily reflect the views and policies of the Asian Development Bank (ADB) or its Board of Governors or the governments they represent.

ADB does not guarantee the accuracy of the data included in this publication and accepts no responsibility for any consequence of their use. The mention of specific companies or products of manufacturers does not imply that they are endorsed or recommended by ADB in preference to others of a similar nature that are not mentioned.

By making any designation of or reference to a particular territory or geographic area in this document, ADB does not intend to make any judgments as to the legal or other status of any territory or area.

This publication is available under the Creative Commons Attribution 3.0 IGO license (CC BY 3.0 IGO) <https://creativecommons.org/licenses/by/3.0/igo/>. By using the content of this publication, you agree to be bound by the terms of this license. For attribution, translations, adaptations, and permissions, please read the provisions and terms of use at <https://www.adb.org/terms-use#openaccess>.

This CC license does not apply to non-ADB copyright materials in this publication. If the material is attributed to another source, please contact the copyright owner or publisher of that source for permission to reproduce it. ADB cannot be held liable for any claims that arise as a result of your use of the material.

Please contact pubsmarketing@adb.org if you have questions or comments with respect to content, or if you wish to obtain copyright permission for your intended use that does not fall within these terms, or for permission to use the ADB logo.

Corrigenda to ADB publications may be found at <http://www.adb.org/publications/corrigenda>.

ABSTRACT

Although agriculture is often considered vulnerable to climate change, recent gridded crop growth modelling intercomparison exercises have found that staple crop yields will be modestly affected by global warming. However, those crop growth models also do not fully reflect impacts of increasing climate extremes. This paper uses global remote sensing-derived yield and agrometeorological reanalysis data to construct a grid cell panel at 0.1-degree resolution for 2003–2015. Regressions that control for grid cell-specific intercepts and time trends, temperature, rainfall, and cloudiness empirically estimate the relationship between yields and precipitation-evapotranspiration extremes for each growing season of rice, wheat, and maize by subregion. Estimated coefficients are applied to projections from an ensemble of global circulation models to project potential losses from climate change. All crops are found as having substantial potential future global yield reductions, but reductions are highest for wheat and maize, with losses most pronounced in Southern Asia and Southern Africa.

Keywords: agriculture, climate change, drought, yield loss

JEL codes: Q12, Q15, Q54, D22

I. BACKGROUND

Agriculture is often considered one of the most vulnerable sectors to the impacts of climate change. Crop production is directly dependent on environmental conditions, with water provided by rainfall and solar radiation through cloud cover as essential inputs, temperatures shaping heat and cold stress, as well as the pace of plant geochemistry and water use, and growing periods defined by seasonal transitions. Early attempts to model the impacts of climate change on agricultural production confirmed the vulnerability of staple crop production to global warming, especially in tropical and subtropical regions. For example, Hasegawa et al. (2022) compiled a database of 8,703 simulations from 202 studies published between 1984 and 2020 of crop growth modelling. Mean results imply yield losses of 14% for rice, 44% for wheat, and 24% for maize in India; and losses of 4% for rice and 10% for maize in the People's Republic of China (PRC) under a high-end emissions scenario by 2050, relative to 2000.

More recent modelling studies, however, find much more limited impact of pronounced climate change. The latest 3b round of the Intersectoral Impact Modelling Intercomparison Project (ISIMIP), which involved 13 crop growth models applied to five downscaled global circulation models, forcing datasets, and tens of thousands of simulations, finds mean yield gains under a high-end emissions scenario for rice and wheat in India and the PRC through late in the century and more modest losses for maize, as well as broader patterns of rice and wheat gains (Orlov et al. 2024). The positive and less damaging effects compared with previous exercises are driven, in part, by increased estimates of the effects of carbon dioxide (CO₂) fertilization, or the increase in photosynthesis that results as CO₂ concentrations rise in high end emissions scenarios. At the same time, the process-based crop growth models used in these exercises have limited ability to replicate the effects of extreme climatic events, such as drought or excessive rainfall.

The models have typically been initially developed to ascertain yield potential, or the maximum yield possible under temperature and solar radiation constraints, without water or nutrient constraints imposed. They are typically further calibrated to replicate crop performance in yield trials under favorable conditions. For example, models used in ISIMIP3b were unable to explain more than 80% of yield variance in major Asian producers' yields of rice, wheat, or maize and consistently overestimated production during drought events (Heinicke et al. 2022). Under climate change, there is general agreement among global circulation models that drought will increase in frequency and intensity (IPCC 2021). Even though in many regions rainfall will increase, as

warmer air can contain more water vapor, higher temperatures increase evaporation and evapotranspiration rates even more, so that conditions are often drier. In addition, climate change makes seasonal variations stronger and amplifies weather variability in many regions, which compounds the effects of higher temperatures. Higher rainfall is often through increased precipitation intensity in short periods, creating additional losses through water stagnation in fields.

While many studies have shown that drought and inundation are damaging to crop yields, few studies have quantified the damage in manner that can be reconciled with climate projections to show global and regional yield loss under climate change. A number of studies have used the standardized precipitation index (e.g., Hendrawan, Komori, and Kim 2023; Vogel et al. 2019), but this index only captures precipitation rather than other determinants of drought related to evapotranspiration. Other prior studies either use country-level data (Matiu, Ankerst, and Menzel 2017), which give few and coarse observations, or data for a single country (e.g., Mohammed et al. 2022; Leng 2021), which reveal only country-specific relationships. Santini et al. (2022) perform somewhat similar analysis to this study by using global spatial yield data, but at 0.5-degree resolution, which is 25 times coarser compared with the data used in the study, and with only dummy representation of extreme events. None of these studies use estimated coefficients with climate projections to show implications of future climate change.

With the availability of global remote sensing-derived crop yield data at 0.1-degree resolution over successive years, along with climatic data for the same units and periods, it becomes possible to empirically estimate the effect of drought and inundation on yield using hundreds of thousands of observations that are much more broadly representative. The empirical estimates can then be applied to geospatial projections of drought and inundation under a high emissions climatic scenario to determine implications for crop production in specific regions. These effects of extreme climatic events can be considered as additional to the effects typically captured in global grided crop modelling exercises, which do not replicate extreme climatic events well and can potentially alter conclusions that climate change impacts on agriculture are modest or beneficial.

II. OBJECTIVES

The purpose of this research is to quantify how the production of rice, wheat, and maize, globally and in specific regions, will be impacted by the increased frequency and intensity of climatic extremes under climate change using large, globally representative, spatial data spanning more than a decade. Such an approach has become possible because of the increasing availability of earth-observation based data for both agricultural production and meteorological conditions. The empirical approach to estimate the effects of extreme events on yields relies on panel data regression, with spatial grid cells as the panel unit. The approach employed uses fixed effects to control for time invariant differences in grid cells and variables that account for common trends over time. Moreover, the preferred specification accounts for grid cell-specific trends over time to eliminate effects of local-level time trends in both independent and dependent variables, so that the analysis is derived from exogenous anomalies. In addition to drought indicators, climatic variables that reflect less extreme changes are included, so as to control for the effects of variables that typically determine yields in gridded crop growth modelling exercises. Additional control variables, such as local CO₂ variations, local air pollution, and irrigation are also tested to determine if they enhance model performance. Once coefficients for climatic extremes are empirically estimated, they are applied to projections of climatic extremes under climate changes to determine overall implications for crop production.

III. METHODS

A. Data

A range of different data sources have been obtained and processed for use in the empirical analysis and future projections.¹ This section begins by presenting the raw datasets and then explaining how they were aggregated and processed. All datasets have been obtained or harmonized to a resolution of 0.1-degree cells, which are approximately 11 kilometers (km) by 11 km at the equator, unless already noted.

¹ The following sections describe the various datasets accessed on 23 July 2024, unless otherwise noted.

1. Raw Data²

Crop yield. Yield data are obtained from the Copernicus Climate Change Project (Wit et al. 2022). This dataset provides insights into the spatio-temporal variations of crop yield at 0.1-degree spatial resolution for different crop types. The data are from a 1-km grid cell fraction of absorbed photosynthetic active radiation (FAPAR) derived from satellite observations on a 10-day basis, interpreted via a crop-specific light use efficiency and temperature function for the reduction assimilation rate of photosynthesis, with growth apportioned between stems, leaves, and grains depending on the growth stage. As FAPAR is the major time-varying observed variable (crop parameters are constant) driving the estimates, water stress is reflected through reductions in leaf area that determine observed FAPAR. These yield data have been confirmed to replicate interannual variability well for areas dominated by the observed crops (Chevuru et al. 2023).

This research focuses on rice, wheat, and maize yields for the period from 2003 to 2015. The crops were chosen for the reason that they are the most important staple food sources globally and account for more than half of all calories consumed by people. This reference period is chosen because data for all variables in the preferred specification and robustness checks are consistently available for this period. More specifically, rice crops often have two cropping seasons within a single campaign year, which is defined as the calendar year of the harvest. The data separate these two growing periods. In the same way, winter and spring wheat are treated as separate within the same campaign year. For each of these crops, data are provided on (i) crop development stage, as a time-series with dekadal (10-day) intervals, indicating whether the crop is in the emergence phase, flowering phase, or at physiological maturity; and (ii) the total weight of storage organs (TWSO), which represents crop yield.

Meteorological. The Copernicus Climate Change Project enables access to agrometeorological indicators derived from reanalysis (AgERA5) at daily and 0.1-degree resolution for use in agro-ecological studies (Boogaard et al. 2020).³ Based on the hourly European Centre for Medium-Range Weather Forecasts (ECMWF) “fifth generation reanalysis for the global climate and weather” (ERA5; Hersbach et al. 2020) data at surface level, the AgERA5 dataset is aggregated to daily time steps and interpolated to the 0.1-degree resolution using regression equations trained on the ECMWF “high resolution atmospheric model.” From the AgERA5 dataset, daily

² Additional data used in robustness checks are described in Appendix 2.

³ C3S (Copernicus Climate Change Service) Climate Data Store. 2020. Agrometeorological Indicators from 1979 to Present Derived from Reanalysis (accessed 10 May 2024).

data on precipitation, temperature, and cloud cover have been obtained. Precipitation represents the total volume of liquid water (cubic millimeter) falling per unit area (square millimeter), temperature refers to maximum air temperature (Kelvin) recorded at 2 meters above the surface, and cloud cover is a dimensionless value indicating the proportion of hours with clouds.

Standardized Precipitation–Evapotranspiration Index. The Standardized Precipitation–Evapotranspiration Index (SPEI) is determined by comparing monthly realization of water balance to long-term average and is normalized to zero mean and unit standard deviation in each cell (Gebrechorkos et al. 2023b). A value of SPEI below zero means drier weather compared to the historic sample, whereas a value above zero means wetter weather. The Centre for Environmental Data Analysis provides historical SPEI data at a monthly and 5 km spatial resolution (Gebrechorkos et al. 2023b). For consistency with available climate projection data, this analysis uses the 6-month period SPEI computed based on monthly precipitation from the Climate Hazards Group InfraRed Precipitation with Station Data (CHIRPS) and potential evapotranspiration from the Global Land Evaporation Amsterdam Model (GLEAM) estimates. This combination shows good agreement with other SPEI databases covering Asian regions (Gebrechorkos et al. 2023a).

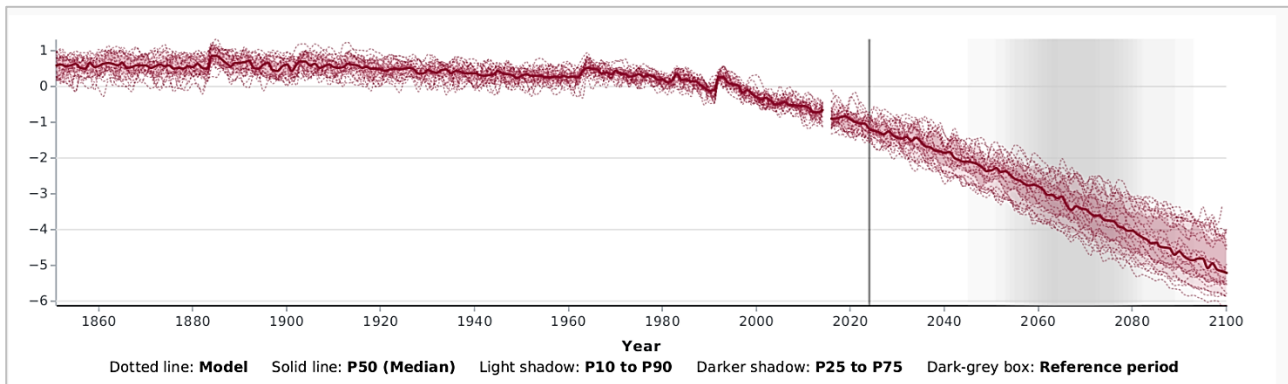
Harvested area. CROPGRIDS provides harvested areas (in hectares) for 173 crops (including maize, wheat, and rice) for the year 2020, at a resolution of 0.05-degree (Tang et al. 2023). It builds on the previously most comprehensive crop area geospatial product from Monfreda, Ramankutty, and Foley (2008) by augmenting it with data from 27 selected published gridded datasets, subnational official statistical data from 52 countries, and 2020 national-level statistics from the Food and Agriculture Organization Corporate Statistical Database (FAOSTAT). This CROPGRIDS harvested area information is used along with the Copernicus Climate Change Project yield data to compute the total production of each crop during projections.

SPEI projection. SPEI projection data are sourced from the Copernicus Interactive Climate Atlas,⁴ which disseminates data that are also underpinning the Sixth Assessment Report of the Intergovernmental Panel on Climate Change. The platform provides monthly projections of the 6-month period SPEI for the years 2030, 2050, and 2090 at a spatial resolution of 1 degree under the high-end emissions scenario used by the Intergovernmental Panel on Climate Change,

⁴ C3S. Copernicus Interactive Climate Atlas (accessed 15 May 2024).

termed Representative Concentration Pathway (RCP) 8.5 (also known as Shared Socioeconomic Pathway 5-8.5). The values are the median of those generated from outputs of 25 different global circulation models run within the Coupled Model Intercomparison Project 6. These data are generated using the Thornthwaite method, with a reference period of 1971–2010 for each grid cell and month. SPEI-6 trends are broadly negative according to these data globally, as evapotranspiration increases outpace precipitation increases where they occur (Figure below).

Figure: Historical and Projected Changes in 6-Month Standardized Precipitation–Evapotranspiration Index



Note: Data are from the Coupled Model Intercomparison Project 6 under a high-end emissions scenario.
 Source: [Copernicus Climate Change Service](#) (accessed 15 May 2024).

Table 1 summarizes the temporal and spatial resolutions, as well as the observation periods, of the different datasets. All data used in the regressions have a 0.1 degree or higher resolution.

Table 1: Resolution Summary and Observation Periods of the Raw Datasets

Dataset	Period	Resolution	
		Time	Spatial
Crop	2003 to 2015	Annual	0.1 degree
Meteorological	2002 to 2015	Daily	0.1 degree
SPEI-6	2002 to 2015	Monthly	5 km
Harvested area	2020	Annual	0.05 degree
SPEI-6 Projection	2030, 2050, 2090	Monthly	1 degree

km = kilometer, SPEI = Standardized Precipitation–Evapotranspiration Index.
 Source: Authors.

2. Data Aggregation

Two aspects are involved in data aggregation. One aspect is to harmonize the grid cell definition so that the data refer to the same geographic area. The other is to reconcile the periods of observation with the growing season for each crop. This process is done separately for each crop type (maize, spring and winter wheat, and wet rice across both growing seasons), as the growing phase, which is central to the analysis, depends on the type of crop.

Crop productivity and climate conditions. The collection of information on meteorological conditions and SPEI comprise climate datasets, while the crop dataset provides information about crop yield and growing phase calendar.

Each grid cell of the crop data is linked to climate dataset grid cells with centroids that fall within the corresponding crop cell. When a crop cell is associated with multiple climate grid cells (as it is the case for the SPEI), the mean of the values across the associated climate cells is used. As a result, each crop cell is associated with daily meteorological data and (average) monthly SPEI data.

Then, for each grid crop cell and for every year from 2003 to 2015, the growing phase is determined (composed by the emergence and flowering stages) to compute the average values of the climate data during this phase.⁵ For the monthly SPEI data, and given that the growing phase is recorded in dekadal (10-day) intervals, a month's value is included in the mean calculation only if the growing phase starts on or before the 20th of the month or ends after the 10th.⁶

The resulting dataset is structured on an annual grid at a spatial resolution of 0.1 degree and covers the period 2003–2015. It provides information on yield productivity and environmental statistics during crop-growing phases for maize, spring and winter wheat, and wet rice across both growing seasons.

Overall quantity of the crop harvested. Every crop data grid cell is matched to harvested area dataset grid cells with centroids that lie within the crop cell. When a crop cell is linked to several

⁵ The growing phases differ depending on the geographic location, year, and the type of crop (maize, rice, and wheat).

⁶ For example, if the growing phase spans from 20 November 2012 to 10 March 2013, values from November, December, January, and February will be included in the mean computation.

harvested area grid cells, the values from these associated cells are summed. This results in a dataset, organized on an annual grid at a spatial resolution of 0.1 degree and covering the period 2003–2015, which provides total harvested quantity of crops (yield × harvested area) for maize, wheat, and wet rice.

Two limits to this approach may be mentioned. First, using the crop data from the Copernicus Climate Change Project enables detailed observation of agricultural productivity at a very fine spatial scale,⁷ but comes with the limitation of incomplete observations. Indeed, some locations that have reported harvested areas according to data from *CROPGRIDS* are missing from the Copernicus dataset, particularly those with smaller harvested areas or mixed cropping composition. As a result, the overall quantity of crop harvested is underestimated. Second, the harvested area dataset only provides information for the year 2020. As a result, the overall quantity of crops harvested is calculated annually by combining yearly productivity time series with the harvested area data from 2020. The implications of these limitations are that (i) losses are more representative of those occurring in more monocropped and larger contiguous conditions than conditions where production is more diversified; and (ii) losses do not account for any dynamism of cropping calendars or crop choice over time to reduce the impacts of SPEI-6 changes. This means that the results are essentially reflecting no climate adaptation.

SPEI projection. Each crop data grid cell centroid is identified to find the nearest centroid from the SPEI projection dataset grid cells. The crop data grid cell is then linked to this closest SPEI projection grid cell. Due to the coarser spatial resolution of the SPEI projection dataset, multiple crop data grid cells may correspond to the same SPEI projection grid cell.

Next, for each crop data grid cell, the average values of the corresponding linked SPEI projection grid cell are computed for the years 2030, 2050, and 2090 during the crop's growing phase, using the growing phase observed in 2015 as a reference. This process provides SPEI projections for the crop data grid cells (during the growing phase) for the years 2030, 2050, and 2090.

⁷ This facilitates a detailed analysis of how meteorological variations influence productivity across locations.

B. Econometric Analysis

The main specification of this study is to estimate the impact of extreme climatic events on crop yield by estimating the following equation for the five crop-seasons presented in the data section:

$$\ln TWSO_{c,t} = X'_{c,t}\beta_i + \alpha_{c0} + \alpha_{c1}t + \varepsilon_{c,t} \quad (1)$$

The subscripts c and t denote the cell and the campaign year (i.e., the calendar year of the harvest), respectively. The dependent variable $\ln TWSO_{c,t}$ is the logarithm of crop yield in cell c at year t . $X_{c,t}$ includes a constant and the environmental conditions in cell c during the growing phase of the year t , with the growing phase specific to the cell c , the year t , and the crop type.

The analysis considers the mean of the maximum temperature and its square ($temp_max_mean$ and $temp_max_mean^2$), the mean of precipitation and its square ($precipitation_mean$ and $precipitation_mean^2$), the mean of cloud cover ($cloud_mean$), and the mean of the SPEI-6 and its square value ($spei_6_mean$ and $spei_6_mean^2$) during the growing phase.

Equation (1) also includes a comprehensive set of fixed effects. The cell fixed effect α_{c0} captures unobserved heterogeneity in crop yield across different cells, such as the possibility that one specific area may be more productive than another. The term $\alpha_{c1}t$ represents cell-specific linear time trends to account for particular developments in crop yield over time within each cell. Last, $\varepsilon_{c,t}$ is the error term.

Quadratic terms are used for temperature and precipitation because crops typically have an optimal level at which yield is maximized, after which yields fall from increases. The same applies to SPEI-6, as a value around 0 indicates typical conditions, negative values indicate more drought, and positive values indicate excess rainfall. Both drought and excess rainfall are expected to reduce yields. Higher cloud cover, ceteris paribus, reduces solar radiation, a key input for photosynthesis, and thus reduces yields. Table 2 shows descriptive statistics for the environmental variables for the five crops: maize, winter wheat, spring wheat, wet rice 1 (for first growing season), and wet rice 2 (for second growing season).

Table 2: Descriptive Statistics

Crop	temp_max_mean (°K)		precipitation_mean (mm)		cloud_mean (fract)		spei_6_mean	
	min	max	min	max	min	max	min	max
Maize	284	312	0	74.2	0	0.33	-2.8	3.7
Winter Wheat	284	310	0	10.62	0	0.15	-2.49	2.5
Spring Wheat	282	310	0	27.52	0	0.21	-2.54	2.52
Wet Rice 1	289	314	0	79.97	0	0.71	-2.81	2.62
Wet Rice 2	288	310	0	31.53	0	0.26	-2.83	2.44

K = Kelvin, mm = millimeters, SPEI = Standardized Precipitation–Evapotranspiration Index.
Source: Authors.

IV. RESULTS

A. Regression Coefficients

Table 3 reports the estimated coefficients of Equation (1) from regressions for the five crop–season combinations. This utilizes the linear estimator proposed by Correia (2016), which is a computationally efficient estimator for large datasets in the presence of multiple fixed effects. To account for the potential autocorrelation of the error terms within cells, the standard errors are clustered at the cell level. It can be noted that all models achieve relatively large explanatory power, with R^2 between 0.87 and 0.94.

The relationship between crop yield and SPEI generally follows an inverse U-shape, with highest yields around SPEI value of 0 and yield reductions as SPEI increases in absolute terms. This corresponds to expectations, as an SPEI of 0 indicates a balance between precipitation and evapotranspiration that is in line with historical averages under which the crops have been cultivated; whereas, negative values indicate drier conditions and positive wetter conditions. It can be expected that agronomic practices and crop varieties are optimized for typical conditions. However, an exception is observed for wet rice during the second growing season, where crop yields increase with SPEI. Rice has a unique production system and is typically cultivated either under irrigation (providing unobserved moisture) or in intense monsoon conditions where rainfall may be excessive, and often is under puddled conditions that improve water retention, which may explain the difference. In addition, crop yields decrease with temperatures, precipitation, and cloud cover. However, wheat demonstrates an exception to this trend, as yields increase with precipitation, provided that precipitation levels remain low. Appendix 1 illustrates the marginal effects of SPEI, temperature and precipitation on crop yield.

Table 3: Estimates of Climate and Weather Effects on Log Global Crop Yields

Statistics	Maize	Winter Wheat	Spring Wheat	Wet Rice 1	Wet Rice 2
spei_6_mean	0.027*** (0.0003)	0.032*** (0.001)	0.080*** (0.001)	-0.007*** (0.0003)	0.033*** (0.001)
spei_6_mean ²	-0.016*** (0.0003)	-0.024*** (0.0004)	-0.059*** (0.001)	-0.004*** (0.0002)	-0.006*** (0.0004)
temp_max_mean	2.307*** (0.027)	3.229*** (0.058)	0.1 (0.070)	5.300*** (0.055)	4.053*** (0.086)
temp_max_mean ²	-0.004*** (0.00005)	-0.006*** (0.0001)	-0.0002** (0.0001)	-0.009*** (0.0001)	-0.007*** (0.0001)
precipitation_mean	-0.006*** (0.0004)	0.153*** (0.002)	0.066*** (0.003)	-0.013*** (0.0005)	0.046*** (0.004)
precipitation_mean ²	-0.00004* (0.00003)	-0.022*** (0.0004)	-0.004*** (0.0005)	0.00005** (0.00002)	-0.005*** (0.0005)
cloud_mean	-0.172** (0.068)	-0.818*** (0.120)	-0.369* (0.199)	-0.577*** (0.031)	-0.759*** (0.056)
Cell fixed effects	Yes	Yes	Yes	Yes	Yes
Cell linear time trends	Yes	Yes	Yes	Yes	Yes
Adjusted R squared	0.87	0.87	0.87	0.93	0.94
Observations	637511	267605	266093	343794	169091

SPEI = Standardized Precipitation–Evapotranspiration Index.

Notes: This table presents the estimation results of Equation (1) for the crops at the head of each column. All regressions include constant, cell-fixed effects, and cell-specific linear time trends. Standard errors clustered by cell appear in parentheses. * p<0.10, ** p<0.05, *** p<0.01. The models are estimated using the Stata reghdfe package developed by Correia (2016).

Source: Authors.

Robustness of the findings. The preferred specification is superior to tested alternatives, including (i) a regression that omits temperature, precipitation, and cloud cover variables; (ii) a regression that uses time and unit dummies, but not time by unit interactions (as Equation 2 below); (iii) a regression that also controls for CO₂ (at 5-degree resolution), irrigation, and air pollution;⁸ and (iv) a regression that also controls for irrigation. The results are presented in Appendix 2. Regression (i) achieves nearly the same R² as the preferred specification, but has larger coefficients, suggesting that small differences in temperature and rainfall are also being captured by the SPEI-6 variables. This makes it difficult to consider as additional to gridded crop growth model results. Regression (ii) has a lower R² than the preferred specification, but similar coefficients. Regression (iii) has implausible coefficients on CO₂ (reverse of the expected sign from CO₂ fertilization) and an R² that is not improved. CO₂ and pollution variables are, however,

⁸ See Appendix 2 for a detailed presentation of these variables.

observed with low granularity and temporal resolution.⁹ Regression (iv) also does not improve R² by including irrigation. Notably, the results, particularly the effect of SPEI on crop yields, remain consistent whether year dummy variables are used instead of cell-specific linear time trends or regressions control for additional factors.

$$\ln TWSO_{c,t} = X'_{c,t}\beta_i + \alpha_{c0} + \alpha_t + \varepsilon_{c,t} \quad (2)$$

Results by subregion. Effects of climatic extremes are estimated on crop yield for different subregions. Table 4 presents the estimated coefficients from Equation (1), derived from regressions for maize, winter wheat, spring wheat, wet rice 1, and wet rice 2 across different subregions of the world. For simplicity, only the estimated coefficients associated with SPEI are reported: column (a) for the variable *spei_6_mean* and column (b) for the variable *spei_6_mean*². However, all regressions include the variables *temp_max_mean*, *temp_max_mean*², *precipitation_mean*, *precipitation_mean*², and *cloud_mean*, as well as the fixed effects described above. The coefficients suggest substantial variation in drought vulnerability for crops cross subregions. For example, maize is more vulnerable to drought in Northern America than the Caribbean, and wheat is more vulnerable in Southern Asia than in Western Asia.

B. Projection of Future Losses Under a High-End Emissions Scenario

To translate the coefficients presented in Table 4 into effects on crop production under climate change, they are used with SPEI-6 projections and historical SPEI-6 observations to calculate effects on yield. These projections take into account both the subregion-specific relationship between yield and SPEI-6¹⁰ and the grid cell-specific changes in SPEI-6 expected under climate change. First, for each grid cell, the historical average SPEI-6 value over 2003–2015 is calculated as a point of reference. Yield loss from reference SPEI-6 is then calculated using linear and squared term coefficients from Table 4. Yield losses under SPEI-6 projected values are subsequently calculated for 2030, 2050, and 2090, from which historical losses are netted, so as to give the effects of climate change on yield. Climate change effects on yield are then multiplied by average historical 2003–2015 production in each grid cell (area of each crop multiplied by the average 2003–2015 yield), summed by subregion, and divided by total historical 2003–2015

⁹ Pollution and irrigation are observed annually, while CO₂ levels are measured at a resolution of 5 degrees. In the case of CO₂ levels, which are observed with much less detail (i.e., have much larger cells) compared to the crop data, the crop data are matched to the CO₂ data using the centroid of the crop data. Specifically, this matching occurs when the centroid of a crop grid cell falls within the area of a CO₂ data cell.

¹⁰ Subregions lacking enough observations for coefficient estimation use global SPEI-6 coefficients from Table 3.

production in each subregion to give relative effects on subregional production. Similar results have been generated by the authors on a country basis and interpolated annually, but are not included in the paper for ease of presentation. The results show high yield vulnerability to the effects of pronounced climate change on precipitation-evapotranspiration extremes (Table 5). In contrast to gridded crop growth model results showing yield gains or modest reductions of only a few percent under a high-end emissions scenario, these results show reductions that exceed 50% for selected subregions and staples within the 21st century. Maize is the crop most vulnerable to changes under climate change, followed by wheat and rice. Losses are highest in tropical and subtropical regions, especially those that have the lowest food security, such as Southern Asia and Southern Africa. The rate of loss appears to accelerate with time, as the 40 or so years from the reference period to 2050 lead to losses that are generally far below additional losses from 2050 to 2090.

Table 4: Estimates of Effects of SPEI-6 on Crop Yields by Subregion

Region	Maize		Winter Wheat		Spring Wheat		Wet Rice 1		Wet Rice 2	
	(a)	(b)	(a)	(b)	(a)	(b)	(a)	(b)	(a)	(b)
	spei6_mean	spei6_mean ²	spei6_mean	spei6_mean ²	spei6_mean	spei6_mean ²	spei6_mean	spei6_mean ²	spei6_mean	spei6_mean ²
Australia and New Zealand					0.159 (0.003)***	-0.035 (0.001)***				
Caribbean	0.000 (0.003)	0.003 (0.003)								
Central America	0.045 (0.003)***	-0.011 (0.002)***								
Central Asia			0.077 (0.003)***	-0.020 (0.002)***	0.116 (0.006)***	0.026 (0.007)***				
Eastern Africa	0.011 (0.002)***	-0.014 (0.002)***								
Eastern Asia	-0.002 (0.001)***	-0.020 (0.001)***	0.025 (0.001)***	-0.014 (0.001)***	0.000 (0.004)	-0.005 (0.004)	-0.016 (0.000)***	-0.012 (0.000)***	0.000 0	-0.010 (0.000)***
Eastern Europe	0.018 (0.001)***	-0.002 (0.001)*	0.013 (0.001)***	-0.005 (0.001)***	0.036 (0.003)***	-0.017 (0.002)***				
Middle Africa										
Northern Africa					0.115 (0.004)***	0.001 (0.002)	0.011 (0.002)***	-0.005 (0.003)**		
Northern America	0.040 (0.001)***	-0.019 (0.000)***	0.126 (0.004)***	-0.041 (0.002)***	0.049 (0.002)***	-0.037 (0.001)***	0.024 (0.002)***	-0.009 (0.001)***		
Northern Europe			0.071 (0.003)***	-0.022 (0.002)***						
South America	0.003 (0.001)***	-0.013 (0.001)***			0.071 (0.003)***	-0.065 (0.001)***	0.020 (0.002)***	0.000 (0.001)		
South-eastern Asia	0.019 (0.001)***	-0.010 (0.001)***					-0.018 (0.001)***	0.001 (0.000)***	0.067 (0.001)***	-0.007 (0.001)***
Southern Africa	-0.006 (0.003)**	-0.023 (0.003)***								
Southern Asia	0.024 (0.001)***	-0.015 (0.001)***	0.008 (0.004)**	-0.031 (0.003)***	0.042 (0.001)***	-0.033 (0.001)***	0.002 (0.001)**	0.000 (0.000)	0.046 (0.002)***	-0.003 (0.002)*
Southern Europe	0.030 (0.002)***	0.001 (0.001)	0.045 (0.002)***	-0.052 (0.002)***	0.023 (0.005)***	-0.027 (0.003)***				
Western Africa	0.011 (0.003)***	-0.006 (0.001)***					0.001 (0.002)	-0.003 (0.002)*		
Western Asia	0.001 (0.005)	0.004 (0.004)	-0.013 (0.001)***	-0.007 (0.001)***	0.124 (0.005)***	-0.088 (0.004)***				
Western Europe	0.025 (0.002)***	0.001 0								

SPEI = Standardized Precipitation–Evapotranspiration Index.

Note: This table presents the estimation results of Equation (1) across different regions of the world for the crops at the head of each column. Only the results associated to the variables `spei_6_mean` (column (a)) and `spei_6_mean2` (column (b)) are displayed. All regressions include constant, `temp_max_mean`, `temp_max_mean2`, `precipitation_mean`, `precipitation_mean2`, `cloud_mean`, as well as cell-fixed effects and cell-specific linear time trends. Standard errors clustered by cell appear in parentheses. * $p < 0.10$, ** $p < 0.05$, *** $p < 0.01$. The models are estimated using the Stata `reghdfe` package developed by Correia (2016). The geographic regions follow the grouping system utilized by the United Nations Statistical Division.

Source: Authors.

Table 5: Effects on Crop Production of Precipitation-Evapotranspiration Extremes Under a High-End Emissions Scenario

Region	Rice Production			Wheat Production			Maize Production		
	2030	2050	2090	2030	2050	2090	2030	2050	2090
Australia and New Zealand				-9.2%	-21.4%	-49.8%			
Caribbean	-4.0%	-8.1%	-19.2%				1.1%	3.2%	10.6%
Central America	-1.3%	-4.8%	-16.6%	-3.7%	-8.9%	-26.3%	-11.0%	-21.8%	-46.9%
Central Asia				-0.6%	-1.3%	-3.8%	-3.5%	-8.9%	-23.8%
Eastern Africa	-3.5%	-10.7%	-33.4%	-0.8%	-3.4%	-14.0%	-4.6%	-13.4%	-40.5%
Eastern Asia	-6.0%	-13.2%	-32.5%	-7.5%	-16.4%	-37.0%	-3.3%	-10.3%	-33.7%
Eastern Europe							-2.6%	-4.4%	-9.7%
Middle Africa	-5.3%	-12.2%	-28.6%				-8.6%	-22.0%	-54.4%
Northern Africa	-5.8%	-12.2%	-30.0%	-11.9%	-19.6%	-36.6%	-2.4%	-7.1%	-23.5%
Northern America	-4.8%	-11.1%	-30.3%	-4.0%	-9.1%	-23.3%	-7.9%	-17.6%	-43.6%
Northern Europe				-4.8%	-15.9%	-46.4%			
South America	-2.9%	-5.2%	-10.0%	-1.4%	-5.6%	-18.0%	-1.9%	-7.7%	-29.1%
South-eastern Asia	4.3%	8.0%	17.5%				-6.4%	-14.5%	-34.3%
Southern Africa				-10.4%	-27.7%	-65.0%	-1.6%	-10.0%	-41.0%
Southern Asia	-0.2%	-0.2%	0.3%	-6.1%	-23.7%	-65.2%	-4.2%	-14.7%	-43.6%
Southern Europe	0.5%	-0.4%	-5.1%	-2.5%	-7.3%	-27.1%	-4.0%	-6.2%	-10.8%
Western Africa	-1.5%	-4.8%	-14.7%				-4.2%	-10.4%	-27.2%
Western Asia				-13.9%	-35.5%	-73.4%	0.3%	1.3%	5.8%
Western Europe				-2.1%	-7.2%	-27.5%	-2.7%	-4.3%	-7.7%

Note: This table presents the difference in yields predicted by coefficients presented in Table 4 applied to ensemble mean values of SPEI-6 under RCP8.5 generated by 25 general circulation models in each future period from yields predicted for the mean 2003–2015 reference period SPEI-6, divided by yields predicted for the mean 2003–2015 reference period. The geographic regions follow the grouping system utilized by the United Nations Statistical Division.

Source: Authors.

The patterns of results are generally consistent with previous findings on the effects of drought and extreme climatic events. Matiu, Ankerst, and Menzel (2017); Hendrawan et al. (2022); and Santini et al. (2022) also empirically find limited impact of drought on rice, compared with wheat and maize. Here, similarly, rice is positively impacted in South-eastern Asia and hardly impacted in Southern Asia, which are two core production breadbaskets. The unique puddled production system for rice, which creates a soil hardpan that reduces percolative water losses; the use of transplanting, which enables adaptation to delayed onset of rains; and the production in intensive wet seasons, may explain the relatively lower vulnerability of rice to drought. In contrast, wheat is negatively impacted in the top producing regions of Eastern Asia and Southern Asia, with impacts especially large in the latter. Large impacts in Eastern Asia are consistent with findings of Yao et al. (2022), while large impacts in Southern Asia are consistent with findings of Kumari et al. (2023).

V. CONCLUSION

It long has been conventional wisdom that agriculture is directly vulnerable to the effects of climate change, especially large levels of change under a high emissions scenario. This research empirically affirms this perspective by taking into account both the subregion-specific relationship between climate extremes and yields and the location-specific predictions of climate extremes under a high-end emissions scenario. In so doing, the regressions find that a quadratic specification of the climate extreme indicator, along with grid cell trends and intercepts, explains a vast majority of yields observed by remote sensing. The research is the first study to estimate yield effects of climate extremes in a manner that is applied to climate projections to show future yield loss globally.

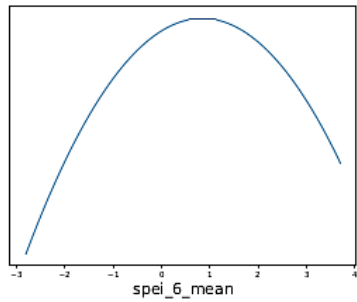
The study's findings of large yield losses under climate change across all three cereals stand in stark contrast to those of recent gridded crop growth modelling studies that yield changes are positive for wheat and rice and modestly negative for maize because of the overwhelming effects of CO₂ fertilization. An attempt to include the effects of CO₂ concentration anomalies finds negative coefficients, rather than positive coefficients consistent with CO₂ fertilization expectations. This may be an artefact of reverse causality, as faster growing crops may deplete CO₂ faster during photosynthesis, creating CO₂ reduction anomalies. It may be noted that the ISIMIP3b yield gains under a high-end emissions scenario are mostly below 10% for rice and below 20% for wheat by 2070 in all regions, which is generally a fraction of the magnitude of losses from this study. As the magnitude of precipitation-evapotranspiration extreme induced losses is far larger than the magnitude of gains found by ISIMIP3b from changes to temperature, rainfall, and CO₂, they imply that crop production is still likely to experience strongly negative effects of climate change. It should be noted that the analysis here is of effects of the changes to the mean of an index of extremes. Effects in future extreme years will be far more pronounced, as what is considered now extreme will be typical in many locations.

APPENDIXES

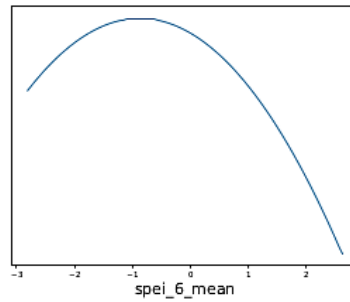
Appendix 1

The results presented in Table 3 are illustrated graphically in Figures A1.1, A1.2 and A1.3. These figures illustrate the marginal effects of the Standardized Precipitation–Evapotranspiration Index (SPEI), temperature and precipitation on crop yield, using the minimum and maximum observed values of these variables (as shown in Table 2) as the relevant lower and upper bounds for analyzing these effects.

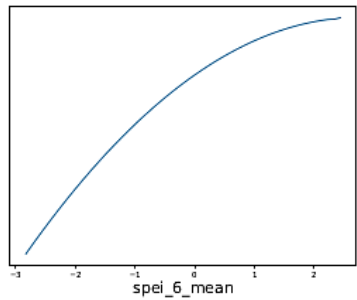
Figure A1.1: Marginal Effects of SPEI on Crop Yields for Various Crops



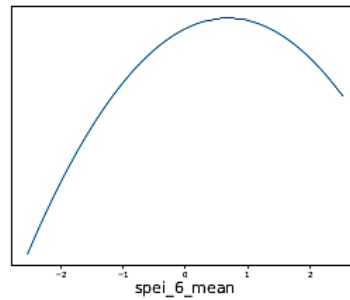
(a) Maize



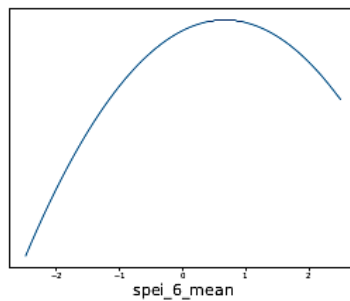
(b) Wet Rice 1



(c) Wet Rice 2



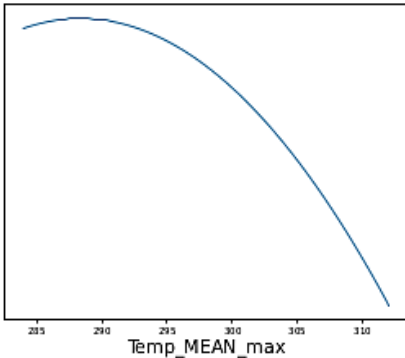
(d) Spring Wheat



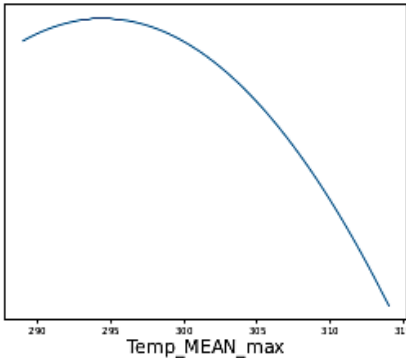
(e) Winter Wheat

SPEI = Standardized Precipitation–Evapotranspiration Index.
Source: Authors.

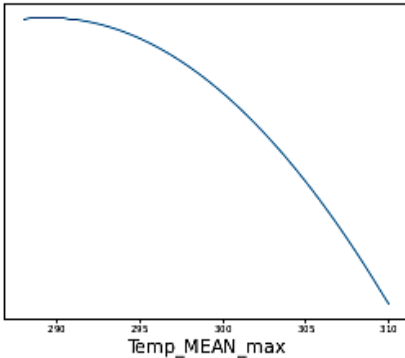
Figure A1.2: Marginal Effects of Temperature (° Kelvin) on Crop Yields for Various Crops



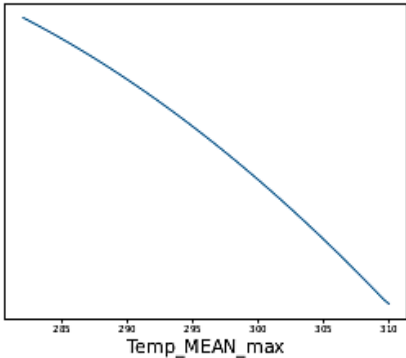
(a) Maize



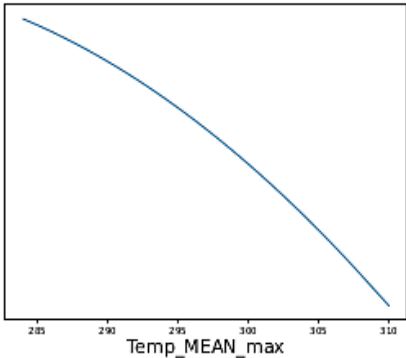
(b) Wet Rice 1



(c) Wet Rice 2



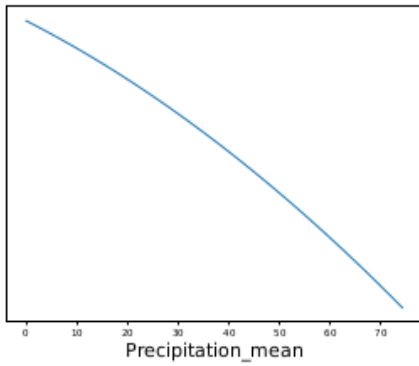
(d) Spring Wheat



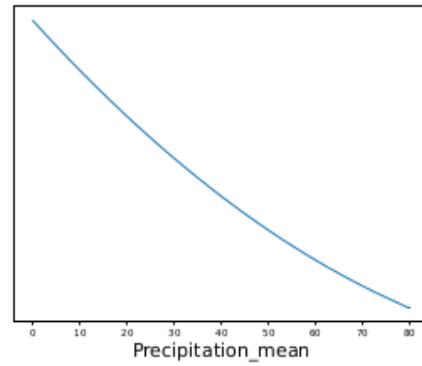
(e) Winter Wheat

Source: Authors.

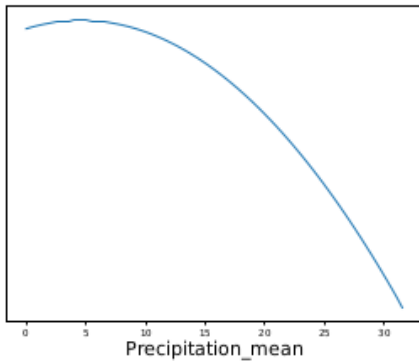
Figure A1.3: Marginal Effects of Precipitation (Millimeters) on Crop Yields for Various Crops



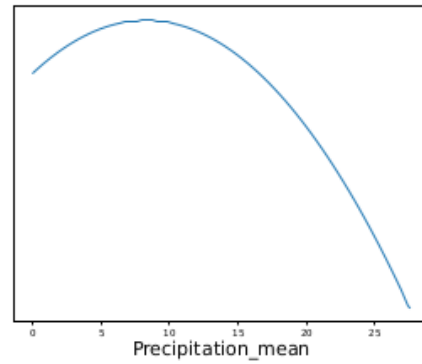
(a) Maize



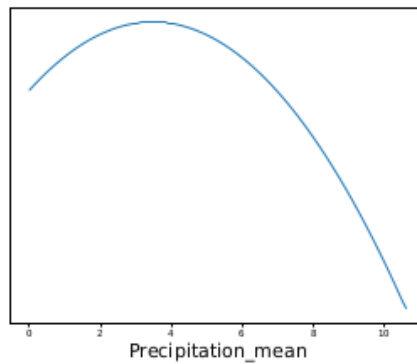
(b) Wet Rice 1



(c) Wet Rice 2



(d) Spring Wheat



(e) Winter Wheat

Source: Authors.

Appendix 2

Equation (2) is estimated considering year dummy variables instead of cell-specific linear time trends, along with cell-fixed effects. Furthermore, this incorporates additional explanatory factors: pollution, irrigation, and carbon dioxide (CO₂) levels.

- Pollution data come from the NASA's Socioeconomic Data and Applications Center (Hammer et al. 2022). This platform offers global annual PM2.5 microgram per cubic meter concentration grids at a spatial resolution of 0.01 degrees (Hammer et al. 2020; Hammer et al. 2022).
- The irrigation dataset provided by Nagaraj et al. (2021) is included. The data are in the form of annual grids at 5 arc-minute spatial resolution and take values between 0 and 2, where 0 represents no irrigation, 1 is low to medium irrigation, 2 is high irrigation.
- CO₂ data comes from the Copernicus Climate Change Project. The column-average dry-air mole fraction of atmospheric carbon dioxide (XCO₂) grids are applied, which are monthly parts per million concentration data at a spatial resolution of 5 degrees.

More specifically, the average irrigation (*irrigation_mean*), the logarithm of the average XCO₂ (*lnxco2_mean*), and the average PM2.5 pollution (*pollution_mean*) during the growing phase are used.

The results are presented in Tables A2.1 through A2.5 for maize, winter wheat, spring wheat, wet rice 1, and wet rice 2, respectively. Columns [1] and [2] show the results using year dummy variables instead of cell-specific linear time trends. Columns [3] and [4] present the results with additional explanatory variables included. Column [5] displays the results from the primary specification used in the main body of the paper for comparison.

Table A2.1: Results for Maize

Statistics	[1]	[2]	[3]	[4]	[5]
spei6_mean	0.032 (0.000)***	0.027 (0.000)***	0.028 (0.000)***	0.027 (0.000)***	0.027 (0.000)***
spei6_mean ²	-0.017 (0.000)***	-0.014 (0.000)***	-0.016 (0.000)***	-0.016 (0.000)***	-0.016 (0.000)***
temp_max_mean		2.252 (0.027)***	2.298 (0.028)***	2.306 (0.027)***	2.307 (0.027)***
temp_max_mean ²		-0.004 (0.000)***	-0.004 (0.000)***	-0.004 (0.000)***	-0.004 (0.000)***
precipitation_mean		-0.005 (0.000)***	0.001 (0.001)	-0.006 (0.000)***	-0.006 (0.000)***
precipitation_mean ²		0 (0.000)**	-0.001 (0.000)***	0 (0.000)*	-0.000 (0.000)*
cloud_mean		-0.375 (0.063)***	-0.366 (0.075)***	-0.168 (0.069)**	-0.172 (0.068)**
irrigation_mean			0 (0.001)	-0.002 (0.001)	
Inxco2_mean			-2.866 (0.080)***		
pollution_mean			0 (0.000)		
Cell fixed effects	Yes	Yes	Yes	Yes	Yes
Cell linear time trends	No	No	Yes	Yes	Yes
Year dummy	Yes	Yes	No	No	No
Adjusted R squared	0.86	0.87	0.87	0.87	0.87
Observation	637,524	637,511	590,407	636,679	637,511

Note: This table presents the estimated effect of environmental variables on maize yield for different specifications. All regressions include constant. In columns [3] to [5] cell-fixed effects and cell-specific linear time trends are included. In columns [1] and [2] cell-fixed effects and time dummy variables are included. Standard errors clustered by cell appear in parentheses. * p<0.10, ** p<0.05, *** p<0.01. The models are estimated using the Stata reghdfe package developed by Correia (2016).

Source: Authors.

Table A2.2: Results for Winter Wheat

Statistics	[1]	[2]	[3]	[4]	[5]
spei6_mean	0.084 (0.001)***	0.045 (0.001)***	0.032 (0.001)***	0.032 (0.001)***	0.032 (0.001)***
spei6_mean ²	-0.028 (0.001)***	-0.023 (0.000)***	-0.025 (0.000)***	-0.024 (0.000)***	-0.024 (0.000)***
temp_max_mean		3.651 (0.059)***	3.333 (0.060)***	3.225 (0.058)***	3.229 (0.058)***
temp_max_mean ²		-0.006 (0.000)***	-0.006 (0.000)***	-0.006 (0.000)***	-0.006 (0.000)***
precipitation_mean		0.131 (0.002)***	0.153 (0.002)***	0.153 (0.002)***	0.153 (0.002)***
precipitation_mean ²		-0.019 (0.000)***	-0.022 (0.000)***	-0.022 (0.000)***	-0.022 (0.000)***
cloud_mean		-0.431 (0.120)***	-0.729 (0.126)***	-0.826 (0.119)***	-0.818 (0.120)***
irrigation_mean			0.02 (0.002)***	0.021 (0.002)***	
Inxco2_mean			-1.567 (0.143)***		
pollution_mean			0.001 (0.000)***		
Cell fixed effects	Yes	Yes	Yes	Yes	Yes
Cell linear time trends	No	No	Yes	Yes	Yes
Year dummy	Yes	Yes	No	No	No
Adjusted R squared	0.85	0.86	0.87	0.87	0.87
Observation	267,605	267,605	261,762	267,605	267,605

Note: This table presents the estimated effect of environmental variables on winter wheat yield for different specifications. All regressions include constant. In columns [3] to [5] cell-fixed effects and cell-specific linear time trends are included. In columns [1] and [2] cell-fixed effects and time dummy variables are included. Standard errors clustered by cell appear in parentheses. * p<0.10, ** p<0.05, *** p<0.01. The models are estimated using the Stata reghdfe package developed by Correia (2016).

Source: Authors.

Table A2.3: Results for Spring Wheat

Statistics	[1]	[2]	[3]	[4]	[5]
spei6_mean	0.114 (0.001)***	0.076 (0.001)***	0.084 (0.001)***	0.08 (0.001)***	0.080 (0.001)***
spei6_mean ²	-0.06 (0.001)***	-0.059 (0.001)***	-0.059 (0.001)***	-0.059 (0.001)***	-0.059 (0.001)***
temp_max_mean		-0.04 (0.075)	0.522 (0.070)***	0.113 (0.070)	0.102 (0.070)
temp_max_mean ²		0 (0.000)	-0.001 (0.000)***	0 (0.000)**	-0.000 (0.000)**
precipitation_mean		0.055 (0.003)***	0.06 (0.003)***	0.066 (0.003)***	0.066 (0.003)***
precipitation_mean ²		-0.004 (0.000)***	-0.004 (0.000)***	-0.004 (0.000)***	-0.004 (0.000)***
cloud_mean		-0.576 (0.190)***	-0.32 (0.246)	-0.387 (0.199)*	-0.369 (0.200)*
irrigation_mean			0.03 (0.004)***	0.027 (0.004)***	
Inxco2_mean			2.343 (0.203)***		
pollution_mean			-0.004 (0.000)***		
Cell fixed effects	Yes	Yes	Yes	Yes	Yes
Cell linear time trends	No	No	Yes	Yes	Yes
Year dummy	Yes	Yes	No	No	No
Adjusted R squared	0.86	0.86	0.87	0.87	0.87
Observation	266,093	266,093	258,321	262,856	266,093

Note: This table presents the estimated effect of environmental variables on spring wheat yield for different specifications. All regressions include constant. In columns [3] to [5] cell-fixed effects and cell-specific linear time trends are included. In columns [1] and [2] cell-fixed effects and time dummy variables are included. Standard errors clustered by cell appear in parentheses. * p<0.10, ** p<0.05, *** p<0.01. The models are estimated using the Stata reghdfe package developed by Correia (2016).

Source: Authors.

Table A2.4: Results for Wet Rice 1

Statistics	[1]	[2]	[3]	[4]	[5]
spei6_mean	-0.039 (0.000)***	-0.013 (0.000)***	-0.006 (0.000)***	-0.007 (0.000)***	-0.007 (0.000)***
spei6_mean ²	-0.002 (0.000)***	-0.003 (0.000)***	-0.004 (0.000)***	-0.005 (0.000)***	-0.004 (0.000)***
temp_max_mean		5.062 (0.055)***	5.275 (0.059)***	5.305 (0.055)***	5.300 (0.055)***
temp_max_mean ²		-0.008 (0.000)***	-0.009 (0.000)***	-0.009 (0.000)***	-0.009 (0.000)***
precipitation_mean		-0.011 (0.000)***	-0.008 (0.001)***	-0.013 (0.000)***	-0.013 (0.000)***
precipitation_mean ²		0 (0.000)	0 (0.000)***	0 (0.000)**	0.000 (0.000)**
cloud_mean		-0.199 (0.029)***	-0.678 (0.034)***	-0.572 (0.031)***	-0.577 (0.031)***
irrigation_mean			-0.002 (0.001)	-0.006 (0.001)***	
Inxco2_mean			-1.608 (0.066)***		
pollution_mean			-0.001 (0.000)***		
Cell fixed effects	Yes	Yes	Yes	Yes	Yes
Cell linear time trends	No	No	Yes	Yes	Yes
Year dummy	Yes	Yes	No	No	No
Adjusted R squared	0.91	0.92	0.93	0.93	0.93
Observation	343,872	343,794	257,330	342,663	343,794

Note: This table presents the estimated effect of environmental variables on wet rice yield (1st growing season) for different specifications. All regressions include constant. In columns [3] to [5] cell-fixed effects and cell-specific linear time trends are included. In columns [1] and [2] cell-fixed effects and time dummy variables are included. Standard errors clustered by cell appear in parentheses. * p<0.10, ** p<0.05, *** p<0.01. The models are estimated using the Stata reghdfe package developed by Correia (2016).

Source: Authors.

Table A2.5: Results for Wet Rice 2

Statistics	[1]	[2]	[3]	[4]	[5]
spei6_mean	0.011 (0.001)***	0.02 (0.001)***	0.039 (0.001)***	0.033 (0.001)***	0.033 (0.001)***
spei6_mean ²	-0.002 (0.000)***	-0.001 (0.000)***	-0.006 (0.000)***	-0.006 (0.000)***	-0.006 (0.000)***
temp_max_mean		4.254 (0.082)***	3.87 (0.076)***	4.076 (0.086)***	4.053 (0.086)***
temp_max_mean ²		-0.007 (0.000)***	-0.006 (0.000)***	-0.007 (0.000)***	-0.007 (0.000)***
precipitation_mean		0.047 (0.004)***	0.057 (0.001)***	0.046 (0.004)***	0.046 (0.004)***
precipitation_mean ²		-0.005 (0.000)***	-0.006 (0.000)***	-0.005 (0.000)***	-0.005 (0.000)***
cloud_mean		-0.788 (0.051)***	-0.696 (0.054)***	-0.752 (0.056)***	-0.759 (0.056)***
irrigation_mean			-0.008 (0.002)***	-0.009 (0.002)***	
Inxco2_mean			-1.973 (0.123)***		
pollution_mean			-0.002 (0.000)***		
Cell fixed effects	Yes	Yes	Yes	Yes	Yes
Cell linear time trends	No	No	Yes	Yes	Yes
Year dummy	Yes	Yes	No	No	No
Adjusted R squared	0.93	0.93	0.94	0.94	0.94
Observation	169,117	169,091	150,592	168,545	169,091

Note: This table presents the estimated effect of environmental variables on wet rice yield (2nd growing season) for different specifications. All regressions include constant. In columns [3] to [5] cell-fixed effects and cell-specific linear time trends are included. In columns [1] and [2] cell-fixed effects and time dummy variables are included. Standard errors clustered by cell appear in parentheses. * p<0.10, ** p<0.05, *** p<0.01. The models are estimated using the Stata reghdfe package developed by Correia (2016).

Source: Authors.

REFERENCES

- C3S (Copernicus Climate Change Service) Climate Data Store. 2020. Agrometeorological Indicators from 1979 to Present Derived from Reanalysis (accessed 10 May 2024).
- C3S. Copernicus Interactive Climate Atlas (accessed 10 May 2024).
- Chevuru, S., A. de Wit, I. Supit, and R. Hutjes. 2023. Copernicus Global Crop Productivity Indicators: An Evaluation Based on Regionally Reported Yields. *Climate Services* 30.
- Correia, S. 2016. *A Feasible Estimator for Linear Models with Multi-Way Fixed Effects*.
- Gebrechorkos, S. et al. 2023a. Global High-Resolution Drought Indices for 1981–2022. *Earth System Science Data* 15.
- Gebrechorkos, S. et al. 2023b. Hydro-JULES: Global High-Resolution Drought Datasets from 1981-2022. NERC EDS Centre for Environmental Data Analysis.
- Hammer, M. S. et al. 2020. Global Estimates and Long-Term Trends of Fine Particulate Matter Concentrations (1998-2018). *Environmental Science & Technology* 54.
- Hammer, M. S. et al. 2022. *Global Annual PM_{2.5} Grids from MODIS, MISR and SeaWiFS Aerosol Optical Depth (AOD), 1998-2019, V4.GL.03*. NASA Socioeconomic Data and Applications Center.
- Hasegawa, T., H. Wakatsuki, , H. Ju et al. 2022. A global dataset for the projected impacts of climate change on four major crops. *Sci Data* 9(58). <https://doi.org/10.1038/s41597-022-01150-7>
- Heinicke, S., K. Frieler, J. Jägermeyr, and M. Mengel. 2022. Global Gridded Crop Models Underestimate Yield Responses to Droughts and Heatwaves. *Environmental Research Letters* 17.
- Hendrawan, V. S. A., W. Kim, Y. Touge, S. Ke, and D. Komori. 2022. A global-scale relationship between crop yield anomaly and multiscalar drought index based on multiple precipitation data. *Environmental Research Letters*, 17(1), 014008. <https://doi.org/10.1088/1748-9326/ac418e>
- Hendrawan, V. S. A., D. Komori, and W. Kim. 2023. Possible Factors Determining Global-Scale Patterns of Crop Yield Sensitivity to Drought. *PLoS ONE* 18.
- Hersbach, H. et al. 2020. The ERA5 Global Reanalysis. *Quarterly Journal of the Royal Meteorological Society* 146.
- IPCC (Intergovernmental Panel on Climate Change). 2021. *Climate Change 2021: The Physical Science Basis*. Contribution of Working Group I to the Sixth Assessment Report of the Intergovernmental Panel on Climate Change.

- Kumari, M., A. Chakraborty, V. Chakravarathi, and P. S. Roy. 2023. Spatio-Temporal Trend of Crop Phenology, SPEI, and Their Interactions over Different Agro-Ecological Regions of India. *Theoretical and Applied Climatology* 154.
- Leng, G. 2021. Maize Yield Loss Risk Under Droughts in Observations and Crop Models in the United States. *Environmental Research Letters* 16.
- Matiu, M., D. P. Ankerst, and A. Menzel. 2017. Interactions Between Temperature and Drought in Global and Regional Crop Yield Variability During 1961-2014. *PLoS ONE* 12.
- Mohammed, S. et al. 2022. Assessing the Impacts of Agricultural Drought (SPI/SPEI) on Maize and Wheat Yields Across Hungary. *Scientific Reports* 12.
- Monfreda, C., N. Ramankutty, and J.A. Foley. 2008. Farming the planet: 2. Geographic distribution of crop areas, yields, physiological types, and net primary production in the year 2000, *Global Biogeochem. Cycles*, 22, GB1022, doi:[10.1029/2007GB002947](https://doi.org/10.1029/2007GB002947).
- Nagaraj, D. et al. 2021. *A New Dataset of Global Irrigation Areas from 2001 to 2015*.
- Orlov, A. et al. 2024. Human Heat Stress Could Offset Potential Economic Benefits of CO₂ Fertilization in Crop Production Under a High end emissions Scenario. *One Earth* 7.
- Santini, M., S. Noce, M. Antonelli, and L. Caporaso. 2022. Complex Drought Patterns Robustly Explain Global Yield Loss for Major Crops. *Scientific Reports* 12.
- Tang, F. H. M. et al. 2023. CROPGRIDS. figshare. Dataset (accessed 15 May 2024).
- Vogel, E. et al. 2019. The Effects of Climate Extremes on Global Agricultural Yields. *Environmental Research Letters* 14.
- Wit, A. et al. 2022. *Crop Productivity and Evapotranspiration Indicators from 2000 to Present Derived from Satellite Observations*. Copernicus Climate Change Service (C3S) Climate Data Store (CDS) (accessed 15 May 2024).
- Yao, N. et al. 2022. Response of Wheat and Maize Growth-Yields to Meteorological and Agricultural Droughts Based on Standardized Precipitation Evapotranspiration Indexes and Soil Moisture Deficit Indexes. *Agricultural Water Management* 266.

Empirically Estimated Impacts of Climate Change on Global Crop Production via Increasing Precipitation–Evapotranspiration Extremes

To assess climate change effects on crop yields, remote sensing–derived yield and agrometeorological reanalysis data are used to construct a panel at 0.1-degree resolution for 2003–2015. Regressions controlling for grid cell–specific intercepts and time trends, temperature, rainfall, and cloudiness estimate the subregional relationships between yields and precipitation–evapotranspiration extremes for rice, wheat, and maize. Results imply that climate change will cause global yield reductions for all crops, with losses highest for wheat and maize, especially in South Asia and Southern Africa.

About the Asian Development Bank

ADB is committed to achieving a prosperous, inclusive, resilient, and sustainable Asia and the Pacific, while sustaining its efforts to eradicate extreme poverty. Established in 1966, it is owned by 69 members —49 from the region. Its main instruments for helping its developing member countries are policy dialogue, loans, equity investments, guarantees, grants, and technical assistance.

